Sonar and Radar SAR Processing for Parking Lot Detection

James Mure-Dubois*, **François Vincent****, **David Bonacci***

*TéSA (Telecommunications for Space and Aeronautics)
14-16, port Saint-Étienne, 31000 Toulouse, France
email: {james.mure-dubois, david.bonacci}@tesa.prd.fr

**Department of Electronics, Optics and Signal, ISAE
1, place Émile Blouin, 31000 Toulouse, France
email: francois.vincent@isae.fr

Abstract: *In this paper, SAR processing algorithms for automotive applications are presented and illustrated on data from non-trivial test scenes. The chosen application is parking lot detection. Laboratory results obtained with a teaching sonar experiment emphasize the resolution improvement introduced with range-Doppler SAR processing. A similar improvement is then confirmed through full scale measurements performed with an automotive radar prototype operating at 77GHz in very close range conditions, typical of parking lot detection. The collected data allows a performance comparison between different SAR processing algorithms for realistic targets.*

1. Introduction

Parking lot detection is a comfort function currently offered to drivers of all categories of passenger cars. While this measurement is usually performed by ultrasound sensors, it has been proposed to use data from side looking radar sensors to realize the same function [1]. In the case of side looking radars/sonars, synthetic aperture radar (SAR) processing can be used to greatly improve the resolution along the direction of motion. However, results published so far concerned simulations or simplified laboratory situations with a small number of point targets [1, 2].

In this paper, two practical systems are used to image scenes containing extended objects: an ultrasound sonar used in the laboratory [3], and a $77\mathrm{GHz}$ prototype for a commercial automotive radar system, used outdoors. In both cases, the resolution improvement brought by low complexity SAR processing such as the range-Doppler algorithm [4] can easily be observed.

In opposition to typical SAR systems, carried by aircraft or satellite, the ranges and range resolutions considered for automotive applications are very short. Therefore, *range migration compensation* (RMC), and particularly the compensation of range curvature has an important role to play in parking lot SAR imaging. Our experiments illustrate the focusing loss when range curvature in not compensated (cf. Fig 5). Nevertheless, SAR processing always brings a significant improvement for parking lot detection, for an additional processing cost that can be kept minimal when using range-Doppler algorithms.

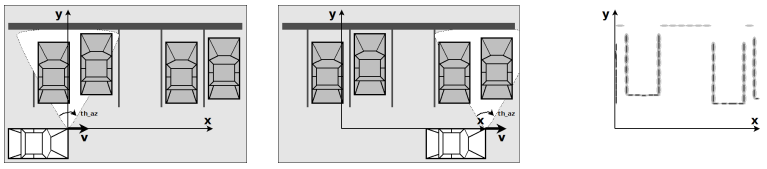

Figure 1: Illustration of SAR imaging geometry and expected result. (left) Carrier position at the beginning of the measurement – (middle) Carrier position at the end of measurement – (right) Final SAR parking lot image

2. SAR and its applications to automotive measurements

As Wu and Zwick [1] note, using existing radar sensors with specifically developed SAR data processing algorithms can provide data needed for parking assistance while keeping the system development and deployment costs low. Fig. 1 illustrates the data acquisition geometry for a typical parking assistance application. This paper illustrates how SAR processing provides the means to greatly enhance the azimuth resolution for the collected data. In order to stay within the constraints of automotive applications, additional filtering operations required by SAR processing should be kept to a minimum. In this paper, the result of lengthy but accurate spatio-temporal SAR processing is compared to two of the least algorithmically expensive solutions for stripmap SAR processing.

Fig. 2b gives an example of acquired data for small scale laboratory scene. While focused in range, the data is blurred in azimuth, since each object was observed many times while it passed through the antenna beam. Following [5], [6] the SAR focusing problem can be formulated by considering that the raw range image is blurred by a *point spread function* (PSF) h, and that the purpose of SAR processing is to provide the required azimuth focus.

At this point, it becomes necessary to distinguish between the *object space* and the *data space* [7]. Data acquisition and the subsequent range focusing perform the transformation from the object space (x, y) to the data space (x, r). Due to the radar displacement along x during the acquisition time, the energy of the response for a point scatterer $\delta(x - x_0, y - y_0)$ is mapped to an hyperbola in the data space: the PSF $h(x - x_0, r; y_0)$ is *two dimensional*. This effect is known as *range migration*, and is very significant in a parking lot application, where very short ranges must be considered. The SAR imaging problem is then to recover the target reflectivity $I(x, y)$ from the SAR measurements $s(x, r)$, and generally involves a matched filter whose role is to compensate as much as possible the effect of the PSF.

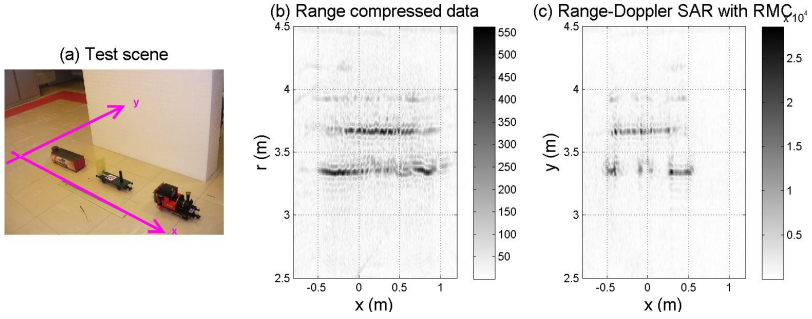

Figure 2: Raw range image obtained for a laboratory scene imaged with a sonar operating at λ=8.5mm.

3. SAR signal processing

For a FMCW radar with minimum frequency f_c and chirp rate α, the emitted chirp is $e(t) = e^{\left(2\pi i\left(f_c t+\alpha t^2\right)\right)}$ where t is the *fast-time*, i.e the time coordinate within the chirp. For a chirp bandwidth B, the chirp rate is $\alpha = B/2T_r$, and T_r is the chirp repetition time. If the radar displacement is sufficiently slow to neglect the changing of r during a ramp, the PSF can be expressed as [1,5]:

$$h\left(x-x_0, r; y_0\right) = \exp\left\{-j\frac{4\pi}{c}\left(f_c+\alpha\frac{r}{c}\right)\sqrt{y_0^2+(x-x_0)^2}\right\} \tag{1}$$

The following paragraphs detail the processing methods used in this article to focus the acquired data into a sharp SAR image $I(x,y)$; the methods are represented schematically in Fig. 3.

3.1. Baseline: spatio-temporal stripmap SAR processing

Since r varies with x and y, a 2D matched filter must be generated for each range bin considered. In spatio-temporal processing stripmap SAR processing, the matched filter $h\left(x-x_0, r; y_0\right)$ for deconvolution is directly applied to the time signal $s(x,r)$ [7]:

$$I\left(x,y\right) = \int_{-\infty}^{\infty}\int_{-\infty}^{\infty} s\left(x',r\right)\cdot h^*\left(x'-x, r; y\right)\, dx'\, dr \tag{2}$$

This processing algorithm gives the most accurate results, as will be illustrated in section 4. Unfortunately, the processing complexity involved is very high, making this method unsuitable for embedded processing inside a vehicle. This method is therefore included only to provide a comparison for the final image quality.

3.2. Range-Doppler algorithm with range curvature compensation

The bandwidth of the PSF is the same for all targets at the same range. Therefore, by taking the Fourier transform along the azimuth dimension, the need to apply a matched filter for all

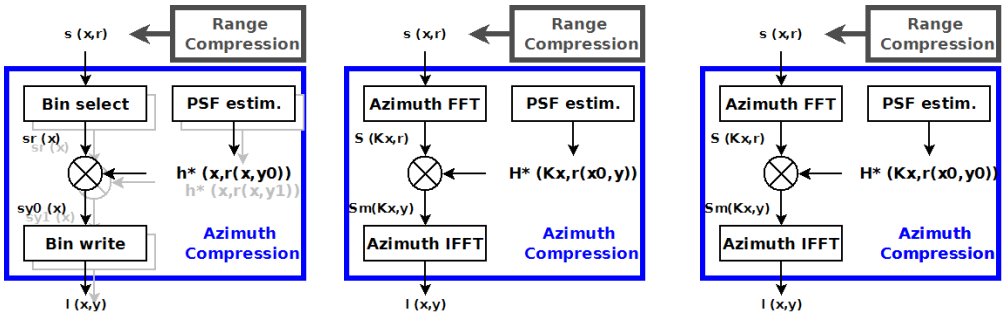

(a) Space-time proc. (b) range-Doppler with RMC (c) Monochrom. range-Doppler

Figure 3: High level description of the processing methods compared in this article.

possible azimuth positions of the target is removed, since the phase histories for targets at different positions in azimuth are mapped to the same regions in the range-Doppler domain [6]. The matched filter in range-Doppler domain is :

$$H^*\left(k_x, r; y_0\right) = \mathscr{F}_x\left\{h^*\left(x - x_0, r; y_0\right)\right\} \tag{3}$$

where $\mathscr{F}_x$ is the Fourier transform along the x direction. For broadside steering, the range dependence of the point spread function h can be incorporated into the phase of the azimuth matched filter applied, by making the assumption that for all targets, the measured range is very similar to the minimum broadside range : $r \approx y_0$. Therefore, the matched filter takes the form $H^*\left(k_x, r\right) = \mathscr{F}_x\left\{h^*\left(x - x_0, r; r\right)\right\}$. The phase of this filter is illustrated in Fig. 4, where the range dependence is clearly apparent.

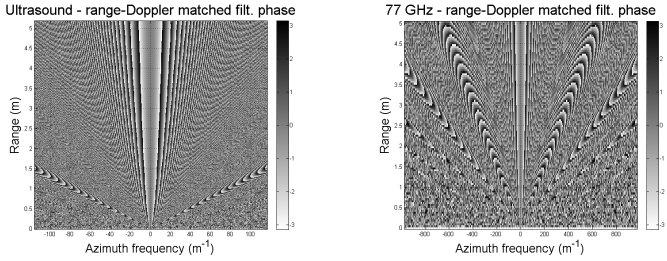

Figure 4: Range-variant phase of the matched filter in range-Doppler processing with range curvature compensation

3.3. Monochromatic range-Doppler stripmap processing

For situations where the range swath imaged is not too wide, it may be desirable to further simplify the matched filter by computing the azimuth matched filter for a single reference range bin, taken at the center y_0 of the scene. This method is labeled as *monochromatic* [7] as only one range bin is considered to define H^*. In embedded systems, this assumption can lead to a significant decrease in memory and processing time required for SAR focusing. The matched filter then becomes :

$$H^*\left(k_x\right) = \mathscr{F}_x\left\{h^*\left(x - x_0, y_0; y_0\right)\right\} \tag{4}$$

This filter will be most efficient for targets located at broadside range y_0, but will lead to defocus errors when the image range is significantly different from the focus range. In section 4, we examine the degradation caused by this approximation by varying the reference range y_0 for the same test scene.

4. Experiments

4.1. Ultrasound system

The ultrasound system used operates at $\lambda = 8.5\mathrm{mm}$ and is therefore a good scale model for automotive radar system operating at 77 GHz [3]. Fig. 5 compares the SAR images obtained

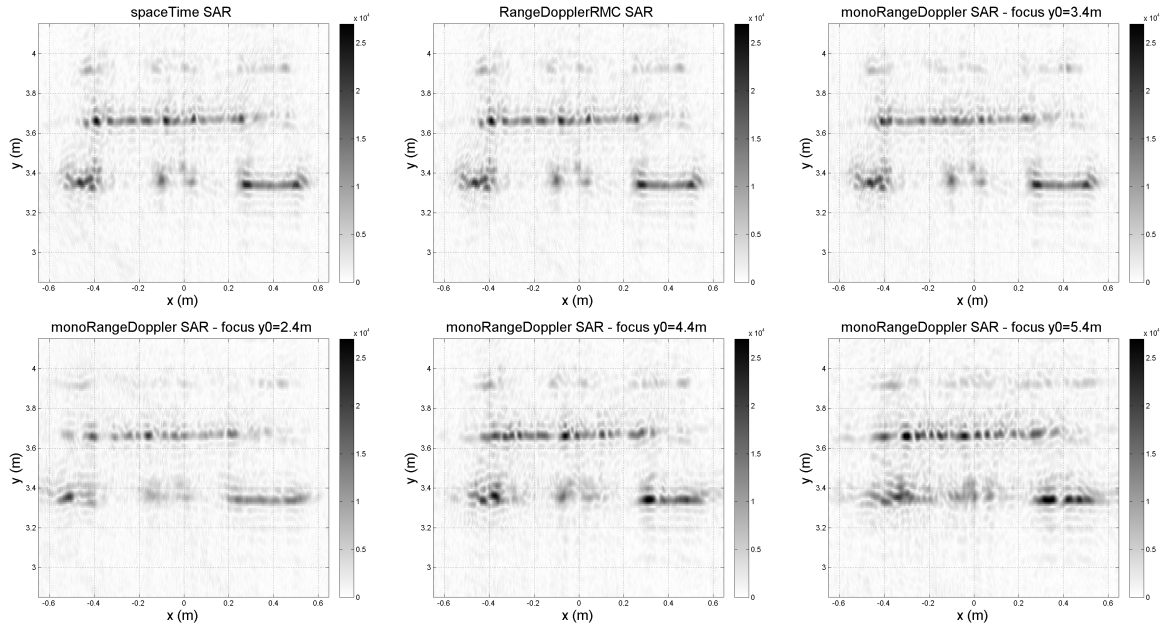

Figure 5: SAR images for extended scene. Notice the monochromatic range-Doppler processing defocus effects.

with space-time processing (top-left), range-Doppler processing with RMC (top-middle), and monochromatic range-Doppler processing for different reference range hypotheses (top-right and bottom row). By comparing these images, one can clearly see that monochromatic range-Doppler processing is a valid approximation for a SAR system with broadside steering when the swath range image is small, but becomes increasingly inaccurate for regions farther away from the reference range y_0. Notice for example that even when the reference range corresponds to the distance to foreground objects (Fig. 5 top-right, $y_0 = 3.35\mathrm{m}$), blurring is noticeable for objects in the background, only $0.4\mathrm{m}$ away from the reference focus. In contrast, range-Doppler processing with range migration compensation provides satisfying azimuth focusing for all regions of the SAR image.

4.2. 77GHz radar system

The $77\mathrm{GHz}$ automotive radar used in our experiments operates at λ=3.9mm and is moved on a rail to ensure a controlled velocity, as shown in Fig. 6(left). For prototype validation, SAR images obtained with the space-time algorithm were computed, as shown in Fig. 6(right). These results indicate that SAR focusing behaves as expected for extended targets in this outdoor scene. More specifically for parking lot detection, SAR processing allows to precisely determine the position and dimension of an obstacle (human being) found in the imaged parking space.

5. Conclusions

In this paper, two low complexity SAR processing methods, suitable for applications such as parking lot detection, were illustrated : range-Doppler processing with RMC, and monochro-

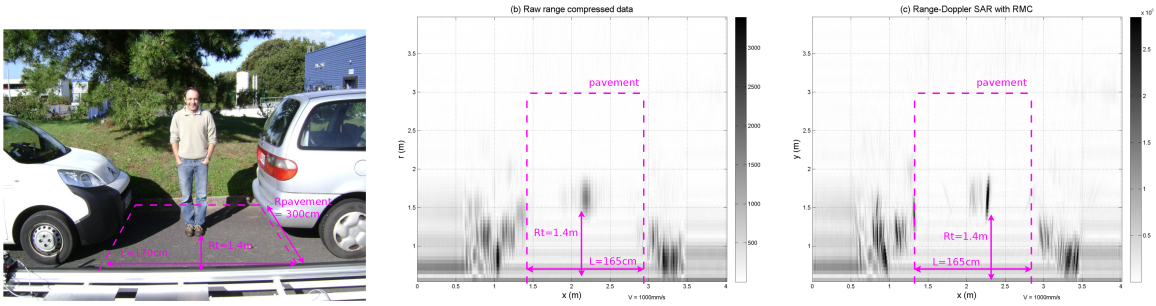

Figure 6: Outdoor test scene (left) for a 77GHz radar experiment. The radar velocity was 1.0m/s. Range compressed data (middle) and azimuth focused image using range-Doppler with RMC (right).

matic range-Doppler. Measurements with a representative ultrasound system have allowed to put in evidence significant defocus effects when monochromatic range-Doppler is used. Nevertheless, its slightly lower complexity and memory consumption could be advantageous in embedded systems with limited resources. When a large range swath is considered, range-Doppler processing with RMC provides satisfying results. To further improve accuracy, SAR processing could use the chirp scaling algorithm (CSA) [8,9] or by ω-k processing [7] (also known as range migration algorithm [8]). However, both of these methods require additional filtering steps and would therefore significantly increase the processing load in an embedded system. Finally, a real scale parking lot experiment with a 77GHz system allowed to verify the improvement brought by SAR processing for an extended scene.

References

[1] H. Wu and T. Zwick, "Automotive SAR for Parking Lot Detection," in *German Microwave Conference, 2009*, mar 2009, pp. 1 –8.

[2] ——, "A novel motion compensation algorithm for automotive SAR : Simulations and experiments," in *German Microwave Conference, 2010*, Berlin, March 2010, pp. 222 –226.

[3] F. Vincent, B. Mouton, E. Chaumette, C. Nouals, and O. Besson, "Synthetic Aperture Radar Demonstration Kit for Signal Processing Education," in *IEEE Int. Conf. on Acoust. Speech Signal Process. ICASSP 2007*, vol. 3, april 2007, pp. III–709 –III–712.

[4] J. de Wit, A. Meta, and P. Hoogeboom, "Modified range-Doppler processing for FM-CW synthetic aperture radar," *IEEE Geosci. Remote Sens. Lett.*, vol. 3, no. 1, pp. 83 – 87, jan 2006.

[5] C. Wu, K. Liu, and M. Jin, "Modeling and a Correlation Algorithm for Spaceborne SAR signals," *IEEE Trans. Aerosp. Electron. Syst.*, vol. AES-18, no. 5, pp. 563 –575, sept. 1982.

[6] J. Munson, D.C. and R. Visentin, "A signal processing view of strip-mapping synthetic aperture radar," *IEEE Trans. Acoust. Speech Signal Process.*, vol. 37, no. 12, pp. 2131 –2147, dec 1989.

[7] R. Bamler, "A comparison of range-Doppler and wavenumber domain SAR focusing algorithms," *IEEE Trans. Geosci. Remote Sens.*, vol. 30, no. 4, pp. 706 –713, jul 1992.

[8] W. G. Carrara, R. S. Goodman, and R. M. Majewski, *Spotlight Synthetic Aperture Radar: Signal Processing Algorithms*. Artech House, 1995.

[9] E. Zaugg and D. Long, "Theory and Application of Motion Compensation for LFM-CW SAR," *IEEE Trans. Geosci. Remote Sens.*, vol. 46, no. 10, pp. 2990 –2998, oct. 2008.